Available online at www.sciencedirect.com
ScienceDirect
Trans. Nonferrous Met. Soc. China 29(2019) 407−415
Transactions of Nonferrous Metals Society of China
www.tnmsc.cn

Kinetics of leaching lithium from *α*-spodumene in enhanced acid treatment using HF/H_2SO_4 as medium

Hui GUO[1,2,3], Hai-zhao YU[1], An-an ZHOU[1], Meng-hua LÜ[1], Qiao WANG[1], Ge KUANG[2], Hai-dong WANG[1]

1. School of Minerals Processing and Bioengineering, Central South University, Changsha 410083, China;
2. Institute of Chemical Technologies, College of Chemical Engineering, Fuzhou University, Fuzhou 350108, China;
3. Department of Chemical Engineering, University of Louisiana at Lafayette, Lafayette 70504, United States

Received 19 January 2018; accepted 24 October 2018

Abstract: An enhanced leaching of Li from *α*-spodumene was carried out using a mixture of hydrofluoric and sulfuric acid (HF/H_2SO_4) as the medium. Based on the optimized leaching conditions, the leaching kinetics of Li was investigated in an ore/HF/H_2SO_4 ratio of 1:3:2 g:mL:mL with leaching temperature ranging from 50 to 100 °C. The results indicate that the leaching kinetics of Li fitted well with a model based on the shrinking core model. In addition, the leaching rate of Li was controlled by chemical reactions and diffusion through the product layers. The apparent activation energy E_a was calculated to be 32.68 kJ/mol. Solid films were formed because of the generation of insoluble products such as cryolithionite ($Na_3Li_2Al_2F_{12}$), cryolite (Na_3AlF_6), calcium fluoride (CaF_2), potassium cryolite (K_2AlF_5), aluminum fluoride (AlF_3), and fluorosilicates (Na_2SiF_6 or $KNaSiF_6$). Furthermore, the effects of the ore/HF ratio and leaching temperature on the leaching behavior of Li, Al and Si were investigated. The results indicate that the ore/HF ratio and leaching temperature could clearly affect the distribution of HF molecules on the leaching of Li, Al and Si, which are important for the selective leaching of Li over Al and Si with this fluorine-based chemical method.

Key words: *α*-spodumene; lithium extraction; leaching kinetics; hydrofluoric acid; fluorine-based chemical method

1 Introduction

Lithium is considered to be a strategic and exceptional element in the preparation of novel energy materials for electric vehicles and portable devices because of its fascinating and rechargeable electro-chemical properties [1,2]. The wide application of Li in ceramics, glass and pharmaceutical fields has also driven the rapid development of efficient processes to extract lithium [3−5].

Traditionally, the extraction of lithium is often emphasized from some brine deposits or some commercial ore resources containing Li [3−7]. Spodumene, which has theoretical formula $LiAlSi_2O_6$, has been widely employed to produce high-purity lithium products because of its high lithium content (up to 8.03% Li_2O). However, spodumene usually exists as *α* phase, which is resistant to most chemicals. Consequently, pre-treatments such as calcination have often been performed at temperatures over 1000 °C to transform *α*-spodumene into a much more reactive *β* phase, which has resulted in a large consumption of energy [8−11].

Here, a novel process with a fluorine-based chemical method was proposed to extract lithium from *α*-spodumene without pre-calcination for phase transformation [12,13]. Combined with the high efficiency of the sulfuric acid method, a hydrofluoric and sulfuric acid (HF/H_2SO_4) mixture was employed to leach lithium from *α*-spodumene and theoretically investigate the reaction mechanism of the fluorine-based chemical method, because the HF molecules were the main reaction forms [14,15].

A series of leaching experiments were conducted, aiming to optimize the leaching conditions of Li. Then, the leaching kinetics of Li was investigated based on the optimal conditions. Empirical models were employed to determine the steps controlling the leaching of Li. Moreover, the obtained residues and corresponding lixiviums were analyzed to understand the leaching behavior of *α*-spodumene in HF/H_2SO_4. Leaching behaviors of some typical elements such as Li, Al and Si

Foundation item: Project (51474237) supported by the National Natural Science Foundation of China
Corresponding author: Hai-dong WANG; Tel: +86-731-88879217; E-mail: joewhd@126.com
DOI: 10.1016/S1003-6326(19)64950-2

were also investigated for different ore/HF ratios (1:1−1:3 g/mL) and leaching temperatures (50−100 °C). The kinetics investigation aims to reveal the mechanism of α-spodumene involved in HF/H_2SO_4, which is important for the selective leaching of Li over Al and Si with this fluorine-based chemical method.

2 Experimental

2.1 Materials and chemicals

The concentrate α-spodumene ore was sampled from Greenbushes, Australia, and contained 5 wt.% Li_2O. Analyses of other major elements were carried out by X-ray fluorescence (XRF) and the results are listed in Table 1. The ore sample was first ground and then sieved with a particle size <75 μm to carry out the leaching experiments.

Table 1 Elemental analysis result of concentrate ore of α-spodumene (wt.%)

Si	Al	Li	O	Na	K	Ca	Fe
32.63	11.43	2.56	41.04	0.35	0.68	0.45	0.54

X-ray diffraction (XRD) analysis (Fig. 1) of the concentrate ore indicated that the ore mainly consists of α-spodumene ($LiAlSi_2O_6$) and is also associated with slight albite ($NaAlSi_3O_8$) and quartz (SiO_2).

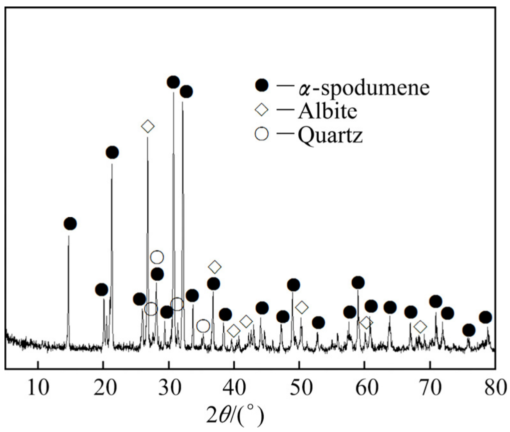

Fig. 1 XRD pattern of α-spodumene ore sample

The chemicals used, HF (40%) and concentrated H_2SO_4 (98%), were both of analytical grades. The concentrated sulfuric acid was pre-diluted with an equal volume of deionized water.

2.2 Procedures

The leaching experiments were performed in a closed Teflon crucible, equipped with a magnetic stirring device and heated by an oil bath. About 10 g of the ore sample was first added into the crucible and then stirred continuously with 1:1 H_2SO_4 and deionized water. Once the desired temperature was reached, the HF was immediately added while still stirring the solution for a certain leaching time. Then, water-leaching was subsequently performed to stop the reaction and obtain kinetics data for different leaching time. The obtained lixivium and insoluble residues were analyzed separately to reveal the leaching behavior and further determine the leaching kinetics of lithium.

2.3 Analytical methods

L was introduced to determine the leaching efficiency of lithium, which was calculated using Eq. (1). Similarly, leaching efficiencies of silicon and aluminum were also determined. In addition, the percentage of insoluble residues (R) was introduced using Eq. (2) to evaluate the generation of the insoluble solid phase:

$$L=\frac{Q_m\cdot V}{10^6 m_{ore}\cdot w}\times 100\% \quad (1)$$

$$R=\frac{m_{res}}{m_{ore}}\times 100\% \quad (2)$$

where Q_m is the concentration of Li in lixivium, mg/L; V is the volume of lixivium, mL; m_{ore} is the mass of the sampled ore, g; w is the mass fraction of lithium in ore sample; m_{res} is the mass of insoluble residues obtained, g.

The lithium contents were determined by atomic absorption spectroscopy (AAS−6800, Shimadzu). Other major elements in lixivium were analyzed using an inductively coupled plasma atomic emission spectrometer (PS−6, Baird). The elemental analysis of the solid phases was determined by XRF (ZSX Primus II, Rigaku). XRD analysis (D/max−2550, Rigaku) was employed to determine major compositions of the solid phases. The morphological changes were observed using a field-emission scanning electron microscope (MIRA3 LMU, TESCAN), which was equipped with an energy-dispersive X-ray spectrometer (EDS; X-Max 20, Oxford Instruments). Fourier-transform infrared spectroscopy (FTIR, IRAffinity−1, Shimadzu) with a frequency range of 400−4000 cm^{-1} was employed to reveal the interaction of lattices in the ore sample or insoluble residues. Nuclear magnetic resonance (NMR) analyses were performed by a Bruker AM400 spectrometer to determine the compositions of lixivium by analyzing the chemical environments of ^{27}Al and ^{19}F.

3 Results and discussion

3.1 Optimal conditions for leaching

A series of leaching experiments were conducted under different conditions, including various ore/HF ratios (1:1.5−1:3.5 g/mL), ore/H_2SO_4 ratios (1:1−

1:3 g/mL), leaching temperatures (50−125 °C), and leaching time, to establish a suitable leaching process to maximize the leaching of lithium and utilization of HF during the acid treatment employing HF/H_2SO_4 as the medium. The results in Fig. 2 indicate that more than 96% of lithium could be leached under optimized conditions: ore/HF/H_2SO_4 ratio of 1:3:2 (g/mL/mL), 100 °C for 3 h with a fixed stirring speed of 150 r/min. A detailed explanation can be found in our previous investigation [13].

It was found from the optimal investigation that the leaching of Li was affected much more significantly by the ore/HF ratio and the leaching temperature than the ore/H_2SO_4 ratio and leaching time. Detailed effects of the ore/HF ratio and leaching temperature on the leaching were further investigated by analyzing the leaching behavior of some typical elements such as Li, Al and Si.

3.2 Leaching behavior of Li, Al and Si

3.2.1 Effect of ore/HF ratio

The above-mentioned experiments show that the ore/HF ratio plays a dominant role in the leaching process, which also affects the generation of insoluble products such as cryolithionite ($Na_3Li_3Al_2F_{12}$), cryolite (Na_3AlF_6), and AlF_3 or fluorosilicates (Na_2SiF_6 or $KNaSiF_6$). Thus, the leaching behavior of elements Li, Al and Si was investigated under different ore/HF ratios, which is important for the efficient utilization of HF and selective leaching of Li over Al and Si.

The results in Fig. 3 indicate that the leaching efficiencies of Li, Al and Si clearly increase with the ore/HF ratio. However, the leaching efficiency differences between Li and Al gradually merge with the addition of HF. While the differences of Si over Li and Al are still clear because of the different reactivity of Si−O, Li−O, and Al−O in the lattice of α-spodumene, it is more difficult to destroy the less reactive [SiO_4], resulting in an incongruent leaching of Li and Al over Si [16]. This incongruent leaching leads to siliceous residues, which could be verified by further XRD and SEM−EDS analyses of the obtained insoluble residues.

3.2.2 Effect of leaching temperature

The leaching temperature, another important factor, clearly affects the reaction, especially for the reactivity of HF molecules and the diffusion of Li. The results in Fig. 4 indicate that the differences among the leaching of Li, Al and Si merge with the increase in temperature.

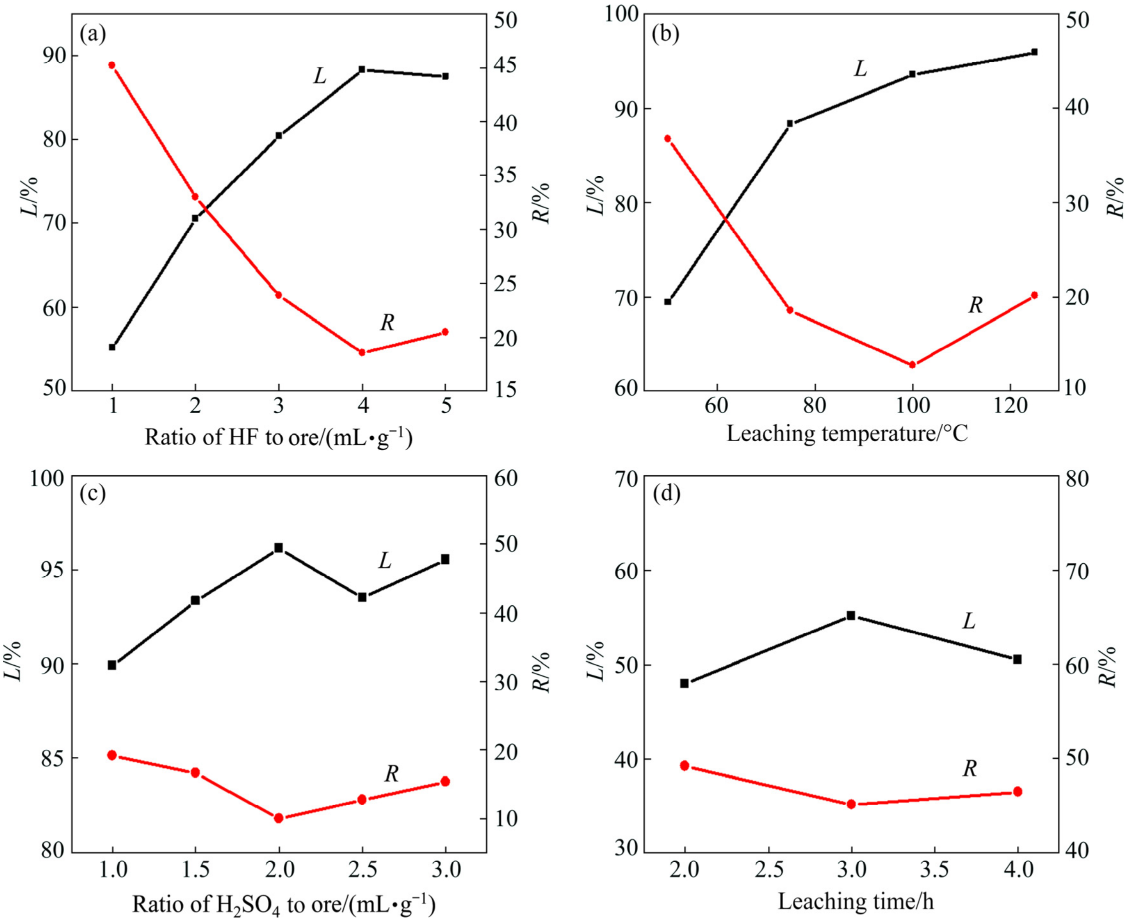

Fig. 2 Effect of different factors on leaching of lithium from α-spodumene using mixed acid HF/H_2SO_4: (a) Ratio of HF/ore; (b) Leaching temperature; (c) Ratio of H_2SO_4/ore; (d) Leaching time

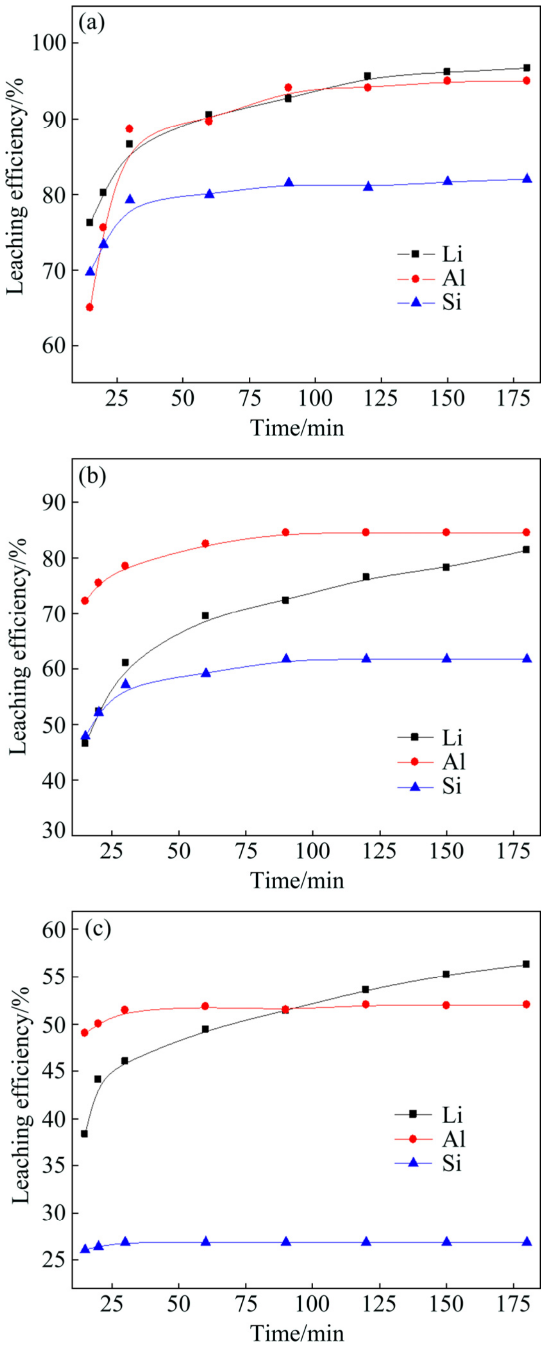

Fig. 3 Effect of ore/HF ratio on leaching rate of Li, Al and Si (ore/H_2SO_4 ratio 1:2 g/mL, 100 °C, stirred at 150 r/min): (a) 1:3 g/mL; (b) 1:2 g/mL; (c) 1:1 g/mL

However, more Li could be converted into lixivium at higher temperatures. The selective leaching of Li and Al over Si is enhanced at 100 °C compared to 75 °C, which can be attributed to the increasing generation of K_2SiF_6 or Na_2SiF_6, resulting in a decrease in retention of Si in liquid.

To briefly summarize, the ore/HF ratio and leaching temperature clearly affect the leaching behavior of Li, Al and Si because of the effects on the distribution of HF molecules to attack Li—O, Al—O or Si—O. Then, the incongruent leaching of Li and Al over Si takes place, which is important for the selective leaching of Li and subsequent purification of lixivium.

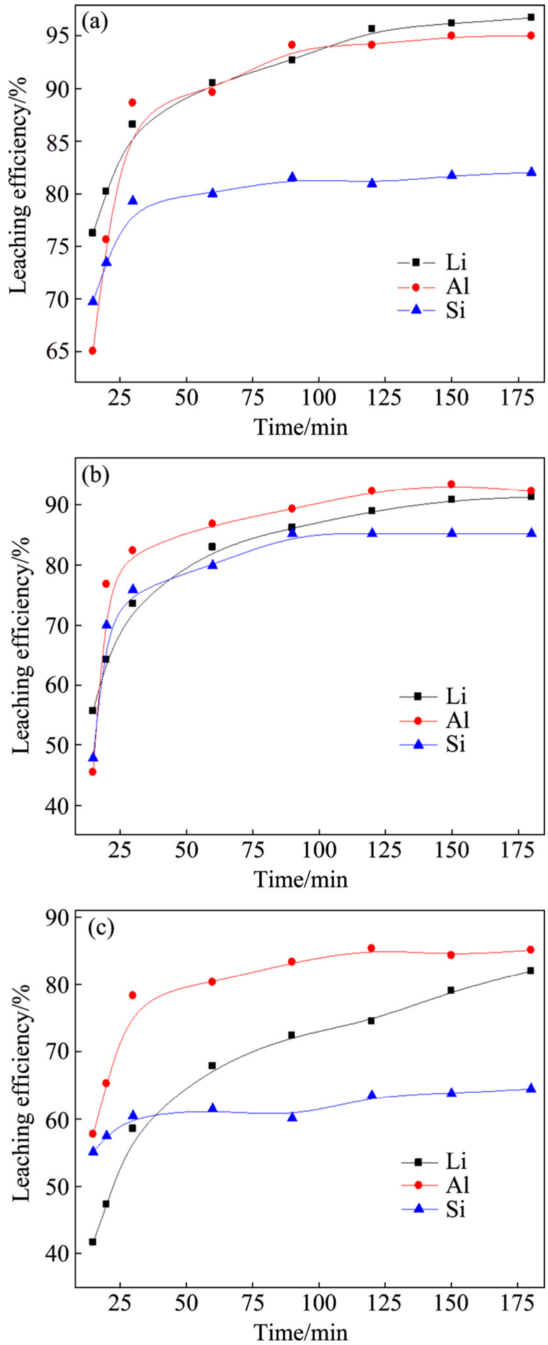

Fig. 4 Effect of leaching temperature on leaching of Li, Al and Si (ore/HF/H_2SO_4 ratio 1:3:2 (g/mL/mL), stirred at 150 r/min): (a) 100 °C; (b) 75 °C; (c) 50 °C

3.3 Analysis of leaching under optimal conditions

3.3.1 Leaching of lithium under optimal conditions

To further understand the leaching behavior, leaching experiments under optimal conditions were conducted at 100 °C in the ore/HF/H_2SO_4 ratio of

1:3:2 (g/mL/mL) for different leaching time. The results in Fig. 5 indicate that the leaching rate of lithium increases with the leaching time; 96% of Li and <10% of R are obtained.

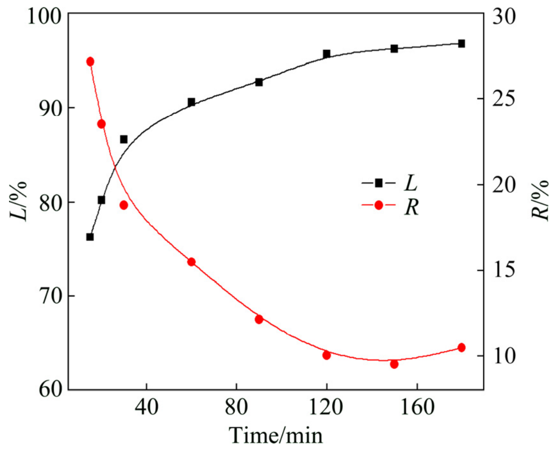

Fig. 5 Leaching of lithium from α-spodumene under optimal conditions (ore/HF/H_2SO_4 ratio 1:3:2 (g/mL/mL), 100 °C, 150 r/min)

3.3.2 XRD analyses of insoluble residues

The disappearance of characteristic peaks in Fig. 6 indicates that α-spodumene and albite are gradually dissolved while the typical peaks of quartz remain, indicating that the preferential dissolving of α-spodumene and albite over quartz occurs and results in a certain selective leaching of Li over Si. Moreover, peaks of some insoluble fluorides can be seen as the leaching progresses. The XRD analyses indicate that most of the major phases of the insoluble residues remain constant from 30 min to 3 h, indicating that the extension of the leaching time slightly affects the leaching process. To maximize the leaching of Li and minimize the generation of insoluble residues, 3 h was employed based on the above-mentioned investigation in Section 3.1.

3.3.3 SEM−EDS analyses of insoluble residues

The SEM images in Fig. 7 indicate that clear morphology changes occur during the leaching process. The original flat surfaces and regular edges of the ore sample gradually turn into porous and irregular residues, which results from the selective attacking of HF molecules onto the preferential sites located on the mineral surfaces or edges. In addition, some insoluble fluorides are generated on the surfaces. Combined with the XRD analyses (Fig. 6), some fluorides (cryolite (Na_3AlF_6), cryolithionite ($Na_3Li_3Al_2F_{12}$), CaF_2, K_2AlF_5, and AlF_3) and fluorosilicates (Na_2SiF_6 or $KNaSiF_6$) are determined. These morphology changes are important for understanding the leaching process and determining the controlling steps in the kinetics investigation, as discussed in Section 3.4.

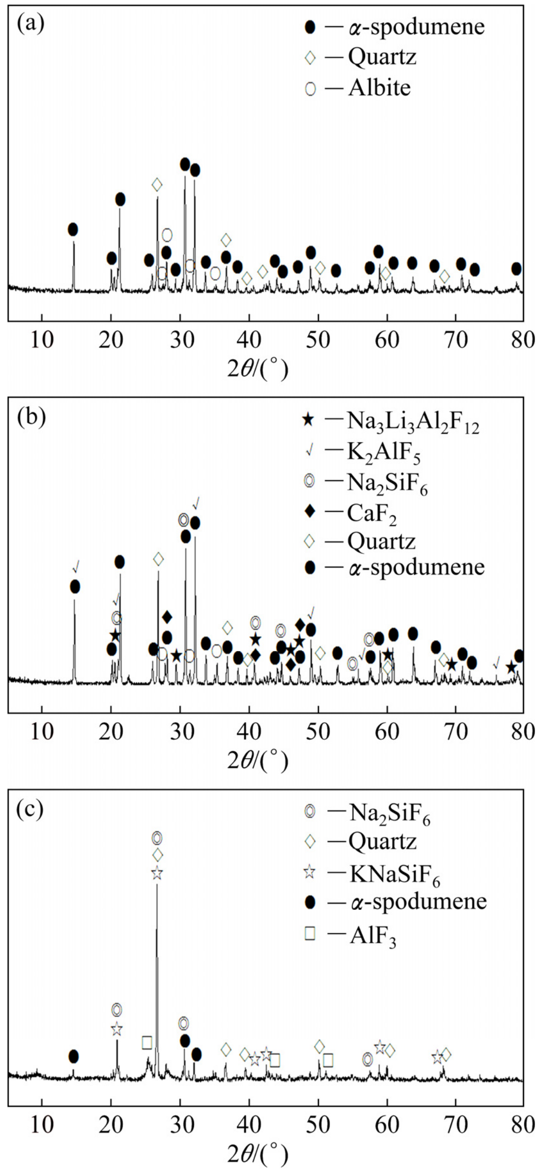

Fig. 6 XRD patterns of residues obtained at different leaching time under optimal conditions (ore/HF/H_2SO_4 ratio 1:3:2 (g/mL/mL), 100 °C, 150 r/min): (a) Ore sample; (b) 15 min; (c) 180 min

3.3.4 FTIR analyses of insoluble residues

Compared to the FTIR spectra of the ore sample in Fig. 8, the M—O bonds at 462.82 cm^{-1} (M represents Li, Al, Ca or other metal atom) dramatically decrease in the insoluble residues [17,18]. The broad peaks at 778.25 and 623.13 cm^{-1} can be attributed to the generation of Si—F—Si [19,20] and Al^{IV}—F, respectively [17]. In addition, the 1088.92 cm^{-1} peak corresponds to the remaining stretching vibration of Si—O in the partially dissolved mineral particles [17]. The peaks at 1648.81 and 3177.07 cm^{-1} are attributed to the bending and stretching vibration of ν_{OH} and H_2O [17], respectively, resulting from the moisture property of SiF_6^{2-}. Moreover, the H^+ introduced by H_2SO_4 increases the amount of Si—OH and Al—OH by protonation, as

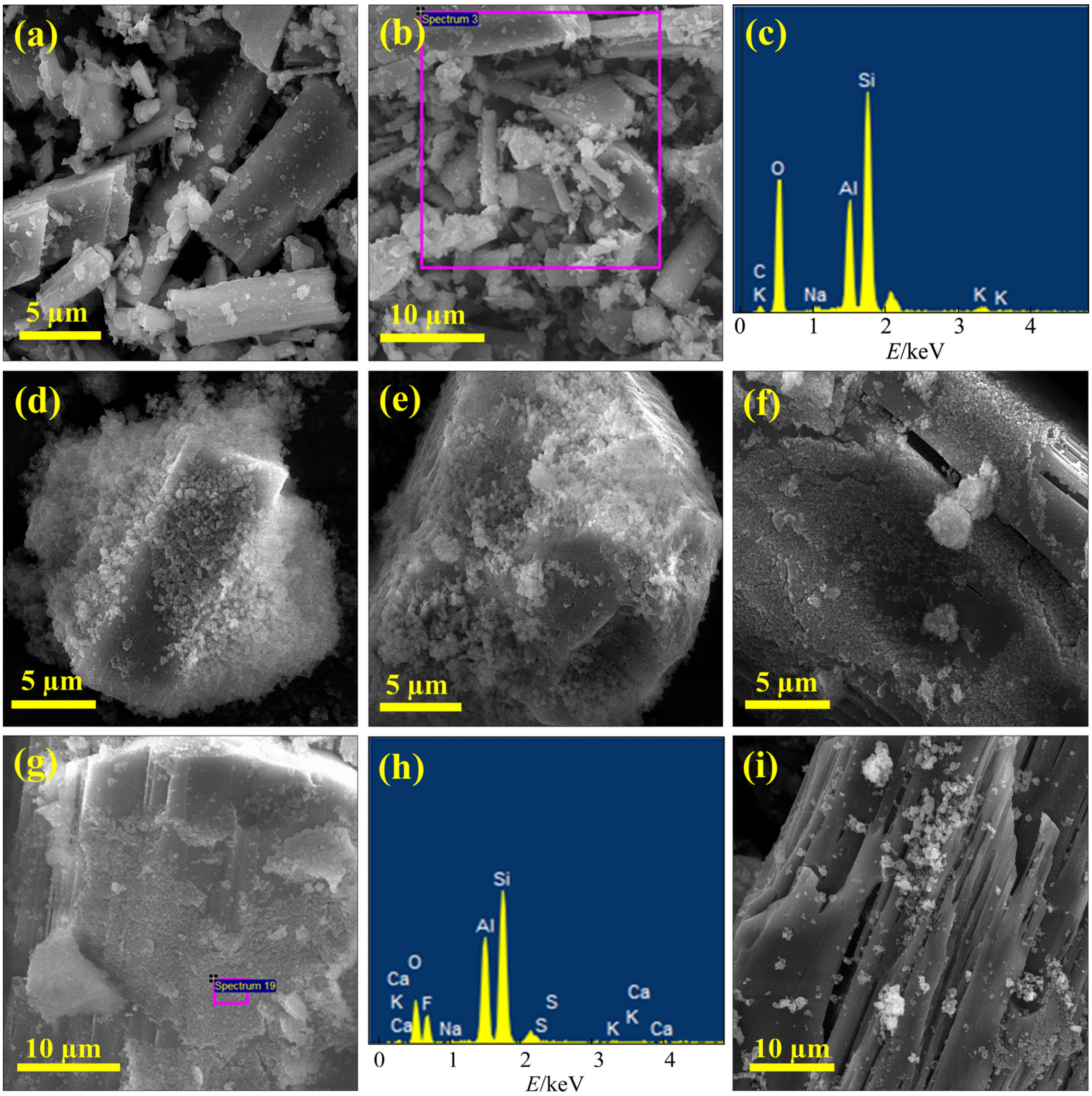

Fig. 7 SEM−EDS images of residues under optimal conditions for different leaching times: (a, b, c) Ore sample; (d, e) 15 min; (f, g, h) 30 min; (i) 180 min

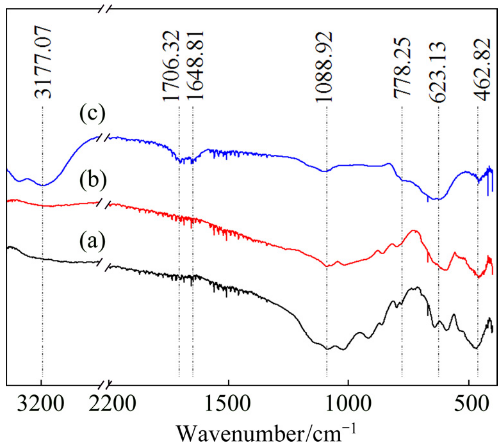

Fig. 8 FTIR spectra of ore sample and insoluble residues under optimal conditions for different dissolution time: (a) Ore sample; (b) 15 min; (c) 180 min

shown in Fig. 9 [14]. Further, the 1706.32 cm^{-1} peak can be assigned to the formation of Na_3AlF_6 [18].

3.3.5 ^{27}Al and ^{19}F NMR analyses of lixivium

The ^{27}Al NMR in Fig. 10 indicates that Al in the lixivium is mainly presented as tetra- (near 80×10^{-6}) or hexa-coordinate aluminum (near zero). However, the resonances slightly shift between 15 and 180 min because of the rapid exchange between F^- and other ligands such as H_3O^+ [21,22]. As the leaching progresses, the coordinated Al gradually shifts from the tetra-coordinate to the six-coordinate because of the different substituted degrees of F^-.

The ^{19}F NMR spectra of the lixivium for 15 and 180 min in Fig. 11 are the same. The decrease in intensity at 180 min is due to the consumption of HF molecules for further reaction. The F in lixivium mainly

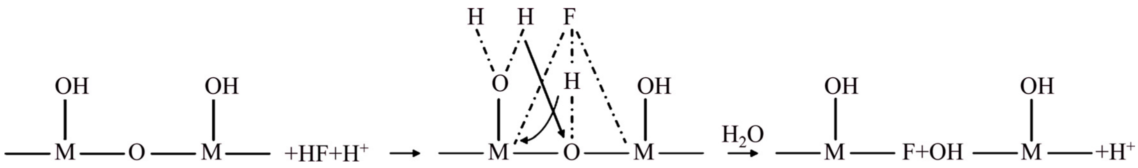

Fig. 9 Protonation of bond lattices by introduced H^+ (M represents Si, Al or other metal elements)

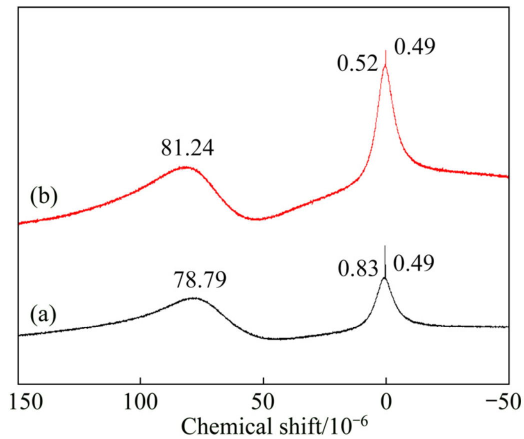

Fig. 10 ^{27}Al NMR spectra of obtained lixivium under optimal conditions (ore/HF/H_2SO_4 ratio 1:3:2 (g/mL/mL), 100 °C): (a) 180 min; (b) 15 min

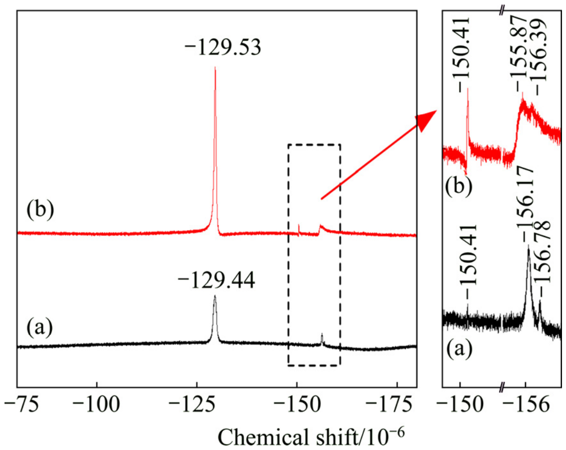

Fig. 11 ^{19}F NMR spectra of obtained lixivium under optimal conditions (ore/HF/H_2SO_4 ratio 1:3:2 (g/mL/mL), 100 °C): (a) 180 min; (b) 15 min

exists as HF/F^-, SiF_6^-, and some complex groups AlF_n^{3-n}, n=1, 2, 3, ⋯, 6 [21−23]. The major compositions of F in lixivium are consistent with the analyses of the corresponding insoluble residues.

3.4 Kinetics analyses

3.4.1 Leaching kinetics of lithium

A previous investigation of the acidizing of sandstone using HF/HCl revealed that the process seemed to fit well with the Freundlich adsorption isotherm equations, and no insoluble products were generated [14]. However, insoluble fluorides such as cryolite (Na_3AlF_6), cryolithionite ($Na_3Li_3Al_2F_{12}$), CaF_2, K_2AlF_5, AlF_3 and fluorosilicates (Na_2SiF_6 or $KNaSiF_6$) are clearly observed in this investigation. In addition, the spodumene composition is clearly different from that of the sandstone, which is mainly composed of carbonate minerals. Here, an intensive investigation was carried out on the leaching kinetics of lithium from α-spodumene in HF/H_2SO_4.

Based on the optimal leaching conditions, the kinetics data under different leaching temperatures (50, 75 and 100 °C) were obtained (Fig. 12(a)) with an ore/HF/H_2SO_4 ratio of 1:3:2 g:mL:mL and a fixed stirring speed of 150 r/min. The investigations of the leaching kinetics could allow for the determination of the controlling steps and evaluation of the effects of different factors on the leaching of Li, which is important for understanding the leaching behavior and providing theoretical constructions for further industrial applications of this fluorine-based chemical method. In addition, the distribution curve of particle size in Fig. 12(b) (D_{50}=6.03 μm, D_{75}=12.45 μm, D_{90}=22.56 μm) was determined using a laser particle size analyzer (LS-POP(6), Omec). The leaching kinetics of lithium in Fig. 12(a) shows that the leaching efficiency clearly increases from 0 to 30 min and then increases slightly from 30 to 180 min.

3.4.2 Model analyses

The process of α-spodumene ore involved in lixiviant HF/H_2SO_4 can be divided into several steps: (1) diffusion of HF molecules and H^+ onto active sites of the mineral surfaces, (2) further reaction with Si—O and Al—O, protonated by H^+, and (3) generation of products and diffusion of Li^+ from the particle surface/product layer into the bulk solution. Meanwhile, other metal ions, K^+, Al^{3+}, etc., can also be leached into the bulk solution with the destruction of the lattice. Here, this dissolution process can be treated as a liquid–solid pseudo-heterogeneous reaction system. Empirical equations based on the shrinking core model with different mechanisms were employed to fit the leaching kinetics data of lithium, aiming to determine the steps controlling the leaching rate of lithium [24−26].

Chemical reaction is

$$1-(1-x)^{1/3}=kt \quad (3)$$

And diffusion through product layer is

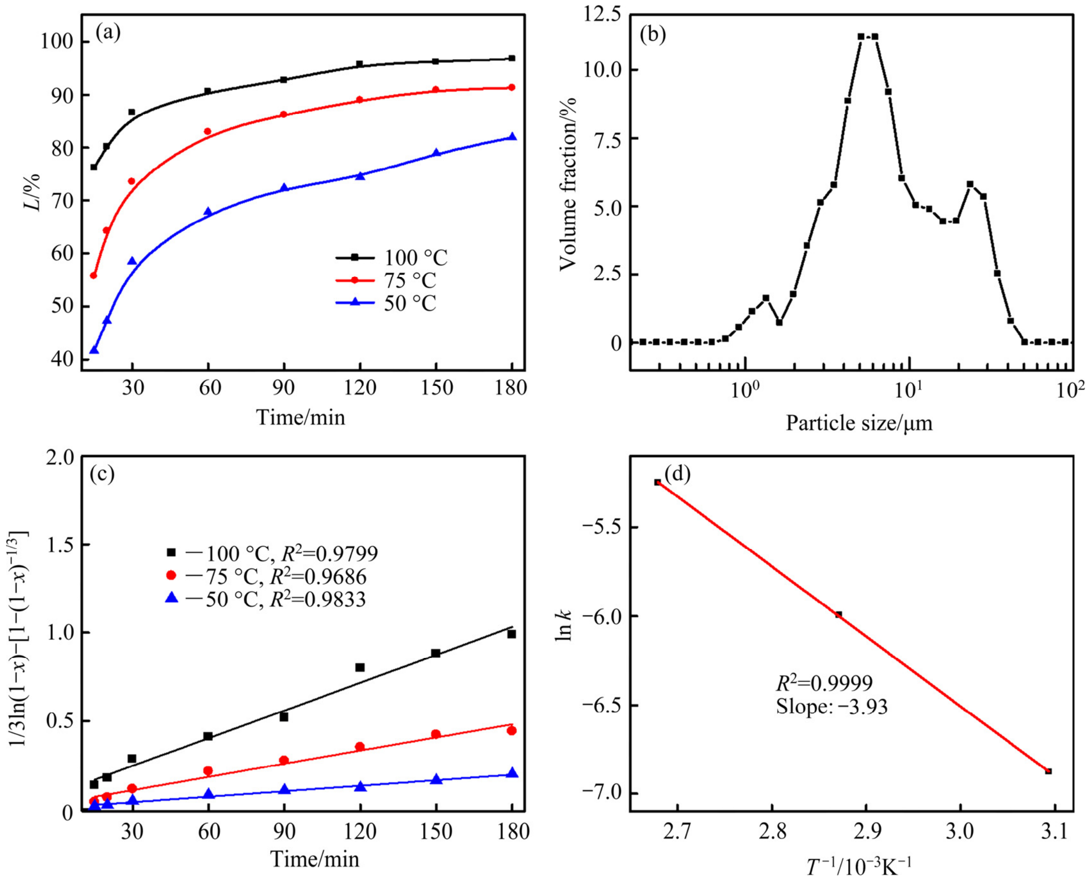

Fig. 12 Kinetics of lithium leaching from α-spodumene in HF/H_2SO_4: (a) Kinetics at different temperatures; (b) Particle size distribution; (c) Fitting results of leaching kinetics data; (d) Arrhenius fitting results

$$1-3(1-x)^{2/3}+2(1-x)=kt \tag{4}$$

However, the fitting results indicate that the kinetics in this leaching system does not fit well with Eqs. (3) and (4). Thus, a developed model based on the shrinking core model was employed, assuming that the reaction rate is controlled by a chemical reaction at the surface and diffusion through the product layers [26,27]:

$$1/3\ln(1-x)-[1-(1-x)^{-1/3}]=kt \tag{5}$$

The results in Fig. 12(c) indicate that the developed model of Eq. (5) actually fits well with the leaching rate of Li, indicating that the leaching rate of Li is controlled by chemical reactions occurring at the surface and diffusion through the insoluble product layers. Moreover, the apparent energy is calculated to be 32.68 kJ/mol (Fig. 12(d)), verifying the fact that the leaching of lithium is controlled by chemical reactions and diffusion through the product layers (14−40 kJ/mol) [28].

4 Conclusions

(1) About 96% of Li was effectively leached from α-spodumene in a HF/H_2SO_4 medium under optimized conditions: ore/HF/H_2SO_4 ratio 1:3:2 (g/mL/mL) at 100 °C for 3 h.

(2) A model developed from the shrinking core model: $1/3\ln(1-x)-[1-(1-x)^{-1/3}]=kt$, was suggested to describe the leaching kinetics of Li, which indicated that the leaching rate of Li is controlled by chemical reactions and diffusion through the solid product layers because of the formation of insoluble fluorides: cryolithionite ($Na_3Li_2Al_2F_{12}$), cryolite (Na_3AlF_6), calcium fluoride (CaF_2), potassium cryolite (K_2AlF_5), aluminum fluoride (AlF_3), and fluorosilicates (Na_2SiF_6 or $KNaSiF_6$).

(3) The selective leaching of Li over Al and Si was affected by the ore/HF ratio and leaching temperature via the influence of the distribution of HF molecules on the leaching of Li, Al and Si.

Acknowledgments

The authors appreciate the Changsha Research Institute of Mining & Metallurgy for elemental analysis.

References

[1] GOODENOUGH J B, PARK K S. The Li-ion rechargeable battery: A perspective [J]. Journal of the American Chemical Society, 2013, 135: 1167−1176.

[2] QIN M L, LIU W M, LIANG S Q, PAN A Q. Facile synthesis of porous $LiNiVO_4$ powder as high-voltage cathode material for lithium-ion batteries [J]. Transactions of Nonferrous Metals Society

of China, 2016, 26: 3232−3237.
[3] KESLER S E, GRUBER P W, MEDINA P A, KEOLEIAN G A, EVERSOND M P, WALLINGTON T J. Global lithium resources: Relative importance of pegmatite, brine and other deposits [J]. Ore Geology Reviews, 2012, 48: 55−69.
[4] MESHRAM P, PANDEY B D, MANKHAND T R. Extraction of lithium from primary and secondary sources by pre-treatment, leaching and separation: A comprehensive review [J]. Hydrometallurgy, 2014, 150: 192−208.
[5] GUO H, KUANG G, WAN H, YANG Y, YU H Z, WANG H D. Enhanced acid treatment to extract lithium from lepidolite with a fluorine-based chemical method [J]. Hydrometallurgy, 2019, 183: 9−19.
[6] CHOUBEY P K, KIM M S, SRIVASTAVA R R, LEE J C, LEE J Y, Advance review on the exploitation of the prominent energy-storage element: Lithium. Part I: From mineral and brine resources [J]. Minerals Engineering, 2016, 89: 119−137.
[7] LI Y, ZHAO Z W, LIU X, Chen X, ZHONG M. Extraction of lithium from salt lake brine by aluminum-based alloys [J]. Transactions of Nonferrous Metals Society of China, 2015, 25: 3484−3489.
[8] KUANG G, LIU Y, LI H, XING S Z, LI F J, GUO H. Extraction of lithium from β-spodumene using sodium sulfate solution [J]. Hydrometallurgy, 2018, 177: 49−56.
[9] CHEN Y, TIAN Q, CHEN B, SHI X, LIAO T. Preparation of lithium carbonate from spodumene by a sodium carbonate autoclave process [J]. Hydrometallurgy, 2011, 109: 43−46.
[10] BARBOSA L, VALENTE G, OROSCO R, GONZALEZ J. Lithium extraction from β-spodumene through chlorination with chlorine gas [J]. Minerals Engineering, 2014, 56: 29−34.
[11] ROSALES G D, RUIZ M C, RODRIGUEZ M H. Novel process for the extraction of lithium from β-spodumene by leaching with HF [J]. Hydrometallurgy, 2014, 147: 1−6.
[12] KUANG G, CHEN Z, GUO H, LI M. Lithium extraction mechanism from α-spodumene by fluorine chemical method [J]. Advanced Materials Research, 2012, 524: 2011−2016.
[13] GUO H, KUANG G, WANG H, YU H, ZHAO X. Investigation of enhanced leaching of lithium from α-spodumene using hydrofluoric and sulfuric acid [J]. Minerals, 2017, 7: 205.
[14] FOGLER H, LUND K, MCCUNE C. Acidization III—The kinetics of the dissolution of sodium and potassium feldspar in HF/HCl acid mixtures [J]. Chemical Engineering Science, 1975, 30: 1325−1332.
[15] KLINE W E, FOGLER H S. Dissolution kinetics: The nature of the particle attack of layered silicates in HF [J]. Chemical Engineering Science, 1981, 36: 871−884.
[16] TERRY B. The acid decomposition of silicate minerals: Part I. Reactivities and modes of dissolution of silicates [J]. Hydrometallurgy, 1983, 10: 135−150.
[17] GUAN J, DI J, YU J, LU Q. Infrared spectra of Zr/Al-pillared montmorillonite mineral material [J]. Journal of the Chinese Ceramic Society, 2005, 33: 220−224. (in Chinese)
[18] DUKE C V A, MILLER J M, CLARK J H, KYBETT A P. 9 MAS NMR and FTIR analysis of the adsorption of alkali metal fluorides onto alumina [J]. Journal of Molecular Catalysis, 1990, 62: 233−242.
[19] HOSHINO D, ADACHI S. Stain etching characteristics of silicon (001) surfaces in aqueous $HF/K_2Cr_2O_7$ solutions [J]. Atherosclerosis, 2007, 154: 139−144.
[20] KABACELIK I, ULUG B. Further investigation on the formation mechanisms of $(NH_4)_2SiF_6$ synthesized by dry etching technique [J]. Applied Surface Science, 2008, 254: 1870−1873.
[21] FINNEY W F, WILSON E, CALLENDER A, MORRIS M D, BECK L W. Reexamination of hexafluorosilicate hydrolysis by ^{19}F NMR and pH measurement [J]. Environmental Science & Technology, 2006, 40: 2572−2577.
[22] MARTINEZ E J M, GIRARDET J L, MORAT C. Multinuclear NMR study of fluoroaluminate complexes in aqueous solution [J]. Inorganic Chemistry, 1996, 35: 706−710.
[23] QIU Z, LIU Y, RU H, ZHENG Q, CHEN Y, ZHU L. Analysis of inorganic fluorine-containing compounds in surface treating agents by ^{19}F NMR [J]. Chinese Journal of Analysis Laboratory, 2013, 32: 70−73. (in Chinese)
[24] TIAN J, YIN J Q, CHI R, RAO G H, JIANG M T, OUYANG K X. Kinetics on leaching rare earth from the weathered crust elution-deposited rare earth ores with ammonium sulfate solution [J]. Hydrometallurgy, 2010, 101: 166−170.
[25] CHI R, ZHU G, XU S, TIAN J, LIU J, XU Z. Kinetics of manganese reduction leaching from weathered rare-earth mud with sodium sulfite [J]. Metallurgical and Materials Transactions B, 2002, 33: 41−46.
[26] DICKINSON C F, HEAL G R. Solid–liquid diffusion controlled rate equations [J]. Thermochimica Acta, 1999, 340: 89−103.
[27] HUANG Y, DOU Z, ZHANG T A, LIU J. Leaching kinetics of rare earth elements and fluoride from mixed rare earth concentrate after roasting with calcium hydroxide and sodium hydroxide [J]. Hydrometallurgy, 2017, 173: 15−21.
[28] DU X L, QIN Y H, WU Z K, CHI R A, WANG C W. Kinetics on leaching of potassium from phosphorus–potassium associated ore in $HCl-H_3PO_4$ media [J]. Transactions of Nonferrous Metals Society of China, 2017, 27: 1870−1877.

α 型锂辉石在混酸介质 HF/H_2SO_4 中浸出锂的动力学

郭 慧[1,2,3]，余海钊[1]，周安安[1]，吕梦华[1]，王 巧[1]，旷 戈[2]，王海东[1]

1. 中南大学 资源加工与生物工程学院，长沙 410083；2. 福州大学 石油化工学院，化学工程技术研究所，福州 350108；
3. Department of Chemical Engineering, University of Louisiana at Lafayette, Lafayette 70504, United States

摘 要：基于单因素条件实验结果，对 α 型锂辉石在混酸介质 HF/H_2SO_4 中不同温度下的浸出动力学进行系统研究。结果表明：在矿物/HF/H_2SO_2 比 1 g : 3 mL : 2 mL、50~100 °C 条件下，锂的浸出过程符合缩核动力学模型，浸出速率主要由表面化学反应以及产物固膜扩散共同控制，表观活化能 E_a 为 32.68 kJ/mol。对固相不溶渣及浸出液组成的分析结果显示：固膜的形成主要由浸出过程中不溶氟化物，如锂钠冰晶石($Na_3Li_2Al_2F_{12}$)、钠冰晶石(Na_3AlF_6)、氟化钙(CaF_2)、钾冰晶石(K_2AlF_5)、氟化铝(AlF_3)及少量氟硅酸盐(Na_2SiF_6、$KNaSiF_6$)的生成所致。此外，氢氟酸添加量及浸出温度可通过影响 HF 分子在浸出锂、铝和硅间的分配而影响浸出过程的选择性。

关键词：α 型锂辉石；矿物提锂；浸出动力学；HF；氟化学法

(Edited by Xiang-qun LI)